Accepted Manuscript

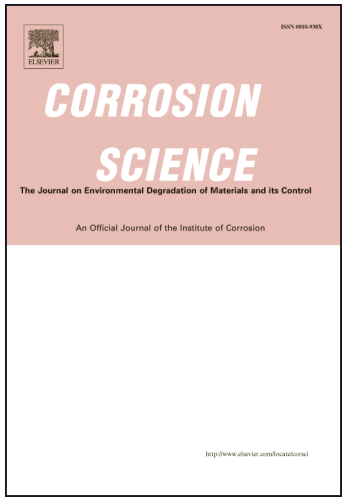

Low apparent valence of Mg during corrosion

Zhiming Shi, Fuyong Cao, Guang-Ling Song, Andrej Atrens

PII: S0010-938X(14)00387-4
DOI: http://dx.doi.org/10.1016/j.corsci.2014.07.060
Reference: CS 5981

To appear in: *Corrosion Science*

Received Date: 30 April 2014
Accepted Date: 29 July 2014

Please cite this article as: Z. Shi, F. Cao, G-L. Song, A. Atrens, Low apparent valence of Mg during corrosion, *Corrosion Science* (2014), doi: http://dx.doi.org/10.1016/j.corsci.2014.07.060

Low apparent valence of Mg during corrosion

Zhiming Shi[1,2,3], Fuyong Cao[1,2], Guang-Ling Song[1], Andrej Atrens[1,2,*]
[*] Corresponding Author, Andrejs.Atrens@uq.edu.au, +61 7 3365 3748

[1] The University of Queensland, Materials Engineering, School of Mechanical and Mining Engineering, Brisbane, Qld 4072, Australia
[2] The University of Queensland, Queensland Centre for Advanced Materials Processing and Manufacturing (AMPAM), Brisbane, Qld 4072, Australia
[3] The University of Queensland, Defence Materials Technology Centre, Brisbane, Qld 4072, Australia

Abstract

Our recent data on Mg corrosion has been reanalysed because of the recent criticism that our previous data analysis was inadequate. Re-analysis leads to similar conclusions as previously. The apparent valence of Mg during corrosion was in each case less than 2.0, and in many cases less than 1.0. Moreover, these values were probably over-estimates. The low values were consistent with the evolving hydrogen gas acting as an insulator, so that the corrosion of parts of the specimen could occur isolated from the electrochemical measurement system.

Keywords: A. Magnesium; B. EIS, B. polarisation, B. weight loss; C. NDE

1. Introduction

The recent paper by King et al [1] considered that type of Mg corrosion data from Electrochemical Impedance Spectroscopy (EIS) that contain an inductive loop. King et al [1] considered a physical model based on adsorbed intermediates in the Mg corrosion reaction, and proposed the equivalent circuit shown in Fig. 1, designated herein the RCL equivalent circuit. Essentially the same equivalent circuit was proposed by Liu et al [2], based on a somewhat different physical model that included the uni-positive Mg^+ ion.

The EIS data analysis proposed by King et al [1] can be understood from Figs. 2(a) and (b), which present typical EIS data for Mg corrosion containing an inductive loop, from Qiao et al [3], for Mg specimen 19 (in the notation of Qiao et al [3]) immersed at the open circuit potential in 3.5% NaCl solution saturated with $Mg(OH)_2$ at 25 °C, for which there was significant micro-galvanic corrosion as evidenced by the corrosion morphology. The definitions of R_s, R_t, and R_P, follow that in King et al [1]. R_s is the solution resistance, R_t is the charge transfer resistance, and R_P is the polarisation resistance. King et al [1] proposed that the polarisation resistance, R_P, should be evaluated as the real part of the impedance, extrapolating the low frequency EIS data to the limit as the frequency (f) approaches zero. This is designated herein as $R_{P,0}$. Such an evaluation of $R_{P,0}$ for Mg corrosion needs a significant *extrapolation* of the measured EIS data.

One possible simple extrapolation is shown by the dashed curve in Figs. 2(a) and (b). The dashed curve shows a simple EIS data fitting of the inductive loop by a semi-circle in the lowest frequency range. Fig. 2(c) presents the equivalent circuit for this simple fitting.

Alternatively, the polarization resistance, R_P could be evaluated at the low frequency limit (typically 10 mHz), designated herein as $R_{P,LF}$. This evaluation is also illustrated in Figs. 2(a) and (b).

From the polarization resistance, R_P, the corrosion current density, i_{corr}, can be evaluated using the Stern-Geary equation [4,5,6]:

$$i_{corr} = \frac{\beta_a \beta_c}{2.3 R_P (\beta_c - \beta_a)} = \frac{B}{R_P} \quad (1)$$

where β_a is the anodic Tafel slope, β_c is the cathodic Tafel slope of an appropriate polarisation curve, and B is a constant involving the Tafel slopes as indicated in Eq(1). The Tafel slopes should be measured from an *iR*-compensated polarisation curve, where i is the current density, and R is the resistance between the specimen and the measuring reference electrode.

Note that i_{corr} is directly proportional to β_a, and note that β_a is typically smaller in magnitude than β_c, for corrosion of Mg in chloride solutions. This means that any error in the measurement of β_a directly converts to a similar error in the measurement of i_{corr}.

If it is assumed that the anodic partial reaction during Mg corrosion involves two electrons as given by

$$Mg \rightarrow Mg^{2+} + 2e^- \quad (2)$$

then, the corrosion current density, i_{corr} (mA cm^{-2}), can be converted to an instantaneous corrosion rate, P_i (mm y^{-1}), using [6,7]:

$$P_i = 22.85\, i_{corr} \quad (3)$$

This paper involves a number of different evaluations of the corrosion rate. Each is listed below.

The proposal by King et al [1] that $R_{P,0}$ is the appropriate measurement method for R_P was quoted to be based on the theoretical analysis by Scully [8], and the experimental study of Lorenz and Mansfield [9]. Lorenz and Mansfield [9] studied pure Fe (Marz grade) in 0.5 M H_2SO_4 containing 10 mM triphenylbenzylphosphonium-chloride ($TPBP^+$). They found that the corrosion rate from the amount of Fe corroded into the solution as measured by atomic adsorption was in good agreement with the corrosion rate evaluated from (i) $R_{P,0}$ evaluated from EIS data (which in their case was the same as $R_{P,LF}$), (ii) R_P calculated from steady-state galvanostatic and potentiostatic polarization curves, and (iii) R_P measured cyclic voltammetrically; but was not in agreement with the corrosion rate evaluated from R_t.

King et al [1] considered that type of Mg corrosion data from EIS that contain an inductive loop, and stated that previous analysis of such EIS data containing an inductive loop had been inadequate. It was therefore important to revisit typical examples of those data.

The aim of this paper was to assess the implication of a reanalysis of our recent EIS data for Mg corrosion [3,6,10,11], based on the suggestions of King et al [1], and in particular if there needed to be any revision of (i) the conclusions in those papers, or (ii) the conclusions regarding the Mg corrosion mechanism made in our recent review [12].

2. HZG Mg

Fig. 3 provides typical data from Qiao et al [3] for HZG Mg immersed at the open circuit potential in 3.5% NaCl solution saturated with $Mg(OH)_2$ at 25 °C for seven days. Qiao et al [3] should be consulted for the complete experimental details. Fig. 3 shows the corrosion rate evaluated from EIS, $P_{i,EIS}$ (full diamonds), measured at daily intervals, as evaluated previously by Qiao et al [3]. $P_{i,EIS}$ was evaluated using Eq(1) and Eq(3), using (i) values of R_t (as defined in Fig. 2) as an appropriate measure of R_P, and (ii) the values of the Tafel slopes, β_a and β_c from the un-*iR*-compensated cathodic polarisation curves measured immediately following each EIS measurement. (These values are in Table 5 in Qiao et al [3]). Each of these cathodic polarisation curves was measured from E_{corr} +30 mV to E_{corr} -300 mV, and the measured cathodic polarisation curve (i.e. measured values of applied potential, E, versus measured values of current density, i) was fitted to

$$i = i_{corr}\left(10^{\frac{E-E_{corr}}{\beta_a}} - 10^{\frac{E-E_{corr}}{\beta_c}}\right) \quad (4)$$

using the software ZView-3.0 (by Scriber Associates Inc. USA) using the non-linear fitting designated as LEV fitting [13,14,15] to yield best fit values of i_{corr}, β_a and β_c.

These values are reproduced in Table 1 (and correspond to the values in Table 5 in Qiao et al [3]). Tafel fitting gave similar values, (see Table 1). The instantaneous corrosion rate, $P_{i,u}$, was evaluated from i_{corr} using Eq(3). The $P_{i,u}$ values have been included in Fig. 3 (as the full circles). Hydrogen evolution was measured throughout the immersion period, and the instantaneous daily corrosion rate, P_H, was evaluated and is also plotted in Fig. 3 (as the full squares) (and is also included in Table 2 for ease of comparison with the other values of the corrosion rate).

After the immersion period, the weight loss for specimen 19 was measured and the corresponding average corrosion rate was

$$P_W = 5.5 \text{ mm y}^{-1} \quad (5)$$

in good agreement with the average corrosion rate evaluated from the total volume of evolved hydrogen

$$P_{AH} = 4.3 \text{ mm y}^{-1} \quad (6)$$

This gives confidence that the instantaneous corrosion rate, P_H, was a good measure of the actual instantaneous corrosion rate, although it was most probably about 20% too small.

The EIS measurements allowed evaluation of the solution resistance, R_s, as shown in Fig. 2. The measured polarisation curves were corrected for *iR* drop. Fig. 4 presents the *iR*-compensated cathodic polarisation curve for Mg specimen 19 from Qiao et al [3]. Table 1 presents the parameters gained from LEV and Tafel fitting of the *iR*-corrected polarisation curves. Table 1 facilitates comparison of these parameters with the ones evaluated from the polarisation curves with no *iR* compensation. Of significance is the fact that the values of the anodic Tafel slope, β_a, from the *iR*-corrected polarisation curves were significantly smaller than those from the polarisation curves with no-*iR*-compensation. This is important because the

corrosion rate is directly related to the value of the anodic Tafel slope, see Eq(1).

Fig. 3 includes the value of the corrosion rate, $P_{i,IRC}$ (open circles) evaluated using LEV fitting of the *iR*-compensated polarisation curves, (and these values are also included in Table 2 for ease of comparison with the other values of the corrosion rate). Typically $P_{i,IRC}$ was similar to (and only slightly larger than) the corresponding corrosion rate evaluated from the polarisation curves with no-*iR*-compensation, $P_{i,u}$.

Fig. 5 presents typical EIS data (data points) and fitting by the RCL equivalent circuit (dashed curve) for Mg specimen 19 of Qiao et al [3] immersed at the open circuit potential in 3.5% NaCl solution saturated with $Mg(OH)_2$ at 25 °C for 1 d. There was reasonable fitting by the RCL equivalent circuit to the experimental data. The values of polarisation resistance, $R_{P,RCL}$ are included in Table 2, as are the corresponding values of the corrosion rate, $P_{i,RCL}$.

The values of $P_{i,RCL}$ are included in Fig. 3 as the full hexagons. These have been evaluated to be in full compliance with the suggestions of King et al [1], and have used the values of the Tafel slopes from the *iR*-corrected polarisation curves measured immediately after the EIS measurements. Thus, each value of $P_{i,RCL}$ must be considered to be as good a measured value as is possible to measure using EIS and polarisation curves, which have been evaluated using the Tafel slopes evaluated by LEV fitting of the *iR*-compensated polarisation curves.

It is instructive to compare the values of $P_{i,RCL}$ (full hexagons in Fig. 3) with the values of $P_{i,EIS}$ (full diamonds in Fig. 5) evaluated previously by Qiao et al [3] using (i) values of R_t (as defined in Fig. 2) as a good measure of R_P, and (ii) the values of the Tafel slopes, β_a and β_c from the non-*iR*-corrected cathodic polarisation curves measured immediately following the EIS measurement. Each value of $P_{i,RCL}$ was typically comparable and only slightly greater than the corresponding value of $P_{i,EIS}$, with the exception of the datum at seven days. In each case the value of $P_{i,RCL}$ was less than the value of P_H and P_W.

As pointed out by King et al [1], the evaluation of R_P requires extrapolation of the EIS data to that corresponding to a frequency of zero. As already mentioned, Fig. 2 illustrates how the data of the inductive loop can be fitted with a simple semi-circle, and the equivalent circuit of Fig. 2(c). This fitting yielded values of $R_{P,sf}$ and the corresponding values of the corrosion rate, $P_{i,sf}$ were included in Table 2 and Fig. 3. These have been evaluated to be in full compliance with the suggestions of King et al [1], and have used the values of the Tafel slopes from the *iR*-compensated polarisation curves measured immediately after the EIS measurements. Each $P_{i,sf}$ value was similar to the corresponding $P_{i,RCL}$ value.

Fig. 6 and Table 3 present the data for a similar evaluation of the data for Mg specimen 28 of Qiao et al [3] immersed at the open circuit potential in 3.5% NaCl solution saturated with $Mg(OH)_2$ at 25 °C for 7 days.

Tables 2 and 3 include values of the apparent valence of Mg evaluated as

$$V_{H,IRC} = \frac{2P_{i,IRC}}{P_H} \tag{7}$$

and

$$V_{H,RCL} = \frac{2P_{i,RCL}}{P_H} \quad (8)$$

based on the assumptions that each of $P_{i,IRC}$ and $P_{i,RCL}$ was a good measure of the amount of the corrosion rate under electrochemical influence, and that P_H was a good measure of the total corrosion rate. Values of apparent valence were in all cases less than 2.0, and were in some cases less than 1.0.

An evaluation of the measurement errors was carried out by Cao et al [6,11]. This indicated that the maximum measurement error was less than 5% in the measurement of both P_W and P_H, whereas the maximum measurement error was 20% in P_i and $P_{i,EIS}$. Thus, there was a significant difference between $P_{i,IRC}$, $P_{i,RCL}$, and P_H and P_W.

3. Mg-RE alloys

Fig. 7 presents re-analysis of typical experimental data from Shi et al [10] for the corrosion of Mg-RE alloys. Shi et al [10] should be consulted for full details of the experiments and experimental data. Immersion tests were carried out for five Mg-RE alloys in the as-cast and solution heat-treated conditions immersed in 3.5% NaCl solution saturated with $Mg(OH)_2$ for 7 days at 25 ± 2 °C. Fig. 7 presents typical data for these alloys. The average corrosion rate measured with weight loss, P_W, was in good agreement with the average corrosion rate evaluated from the total evolved hydrogen, P_{AH}. This indicates that the corrosion rate evaluated from hydrogen evolution was a good measure of the corrosion rate.

The instantaneous corrosion rate, $P_{H6.5}$, was evaluated corresponding to day 6.5 from the slope of the hydrogen evolution volume versus time data. $P_{H6.5}$ was in all cases in Fig. 7 greater than the average corrosion rate, P_{AH}, reflecting the fact that the corrosion rate increased somewhat during the immersion test.

The corrosion rate, $P_{i,u}$, was evaluated by Tafel extrapolation of the polarisation curves measured during the seventh day of immersion with no *iR* compensation. $P_{i,u}$ was consistently less than $P_{H6.5}$, see Fig. 7.

EIS were measured during the seventh day of immersion. The corresponding corrosion rate, $P_{i,EIS,LF}$, was evaluated from (i) $R_{P,LF}$ as defined in Fig. 2, as the value of R_P at the lowest frequency measured (10 mHz) of the EIS data, and (ii) the Tafel slopes of the polarisation curves measured during the seventh day of immersion with no *iR* compensation.

The values of P_W, P_{AH}, $P_{H6.5}$, $P_{i,u}$ and $P_{i,EIS,LF}$ correspond to the values evaluated by Shi et al [10].

The corrosion rate, $P_{i,RCL}$, was evaluated from (i) $R_{P,0}$ as defined in Fig. 2, as the value of R_P extrapolated to zero frequency with the EIS data fitted by the RCL equivalent circuit (Fig. 1), and (ii) the Tafel slopes of the *iR*-corrected polarisation curves that were measured during the seventh day of immersion. Table 4 lists the values of the parameters.

The corrosion rates measured from the EIS data using the RCL equivalent circuit, $P_{i,RCL}$, were each significantly less than $P_{H6.5}$.

Fig. 8 shows a typical time series comparison for typical Mg-RE alloys immersed in 3.5%

NaCl solution saturated with $Mg(OH)_2$ for 7 days at 25 ± 2 °C. The instantaneous corrosion rate evaluated from the evolving hydrogen, P_H is compared with the corrosion rate evaluated from the EIS data, $P_{i,RCL}$, from (i) the value of $R_{P,0}$ extrapolated to zero frequency with the EIS data fitted by the RCL equivalent circuit (Fig. 1) and (ii) the Tafel slopes of the *iR*-corrected polarisation curves that were measured during the seventh day of immersion.

The instantaneous corrosion rates from the EIS measurements, $P_{i,RCL}$, were typically always less than the corrosion rate measured from hydrogen evolution, P_H. Similar to the conclusions reached above, these differences were significant.

4. Mg-X alloys

Figs. 9 and 10 present an analysis for the data of Cao et al [11] for the corrosion of Mg-X alloys that was similar to that presented above for the data of Shi et al [10] for the corrosion of the Mg-RE alloys. The conclusions were similar: (i) in Fig. 9 the instantaneous corrosion rates measured from the EIS data fitted to the RCL equivalent circuit, $P_{i,RCL}$, were each significantly less than $P_{H6.5}$; and (ii) in Fig. 10 the instantaneous corrosion rates from the EIS measurements, $P_{i,RCL}$, were always significantly smaller than the corrosion rate measured from hydrogen evolution, P_H. Again these differences were significant in comparison with the measurement errors.

Table 5 includes values of the apparent valence of Mg for the Mg-RE and Mg-X alloys evaluated from Eq.(8). Values of apparent valence were in all cases less than 2.0, and were in many cases less than 1.0.

5. UP Mg

Cao et al [6] studied the corrosion of specimens from two ingots (designated A and B) of ultra-high-purity (UP) Mg immersed at the open circuit potential in 3.5% NaCl solution saturated with $Mg(OH)_2$ at 25 °C for 14 days, using the approach as described in Shi et al [7]. The paper by Cao et al [6] should be consulted for the full details of the experimental methods and results. Corrosion was characterised by measurements of the volume of hydrogen evolved for the duration of the immersion period, EIS measurements at approximately daily intervals, cathodic polarisation curves measured after 14 days immersion, and weight loss.

Each cathodic polarisation curve was measured from E_{corr} +30 mV to E_{corr} -300 mV. LEV fitting [13,14,15] of the measured cathodic polarisation curve yielded best-fit values of i_{corr}, β_a and β_c.

The hydrogen evolution volume increased approximately linearly with immersion time indicating that the corrosion rate was approximately constant with immersion time. The average corrosion rate evaluated from the total volume of evolved hydrogen, P_{AH}, was in all cases smaller than (and in many cases considerably smaller than) the average corrosion rate evaluated with weight loss, P_W, attributed to some dissolution of hydrogen in the Mg specimen material.

Fig. 11(a) presents typical EIS data showing only two capacitive loops, whereas Fig. 11(b) presents EIS data showing two capacitive loops and an inductive loop.

Figs. 12 and 13 show representative data. Fig. 12(a) shows corrosion rate data for specimens A1 and A2 from ingot A. The EIS data for the 13th day for A1 corresponded to the type illustrated in Fig. 11(b), for which the polarisation resistance, R_P, was evaluated as indicated as $R_{P,LF}$. All the other EIS data for specimens A1 and A2 corresponded to that illustrated in Fig. 11(a), for which the polarisation resistance, R_P, was evaluated as indicated as $R_{P,0}$. Fig. 12(a) shows the corresponding values of the instantaneous corrosion rate, $P_{i,EIS,UP}$, plotted as a function of time, and these values have been included in Table 6. $P_{i,EIS,UP}$ was evaluated using the Tafel slopes evaluated from the *iR*-corrected polarisation curves, given in Table 7. For comparison, also plotted are the values of the instantaneous corrosion rates evaluated from the hydrogen evolution, P_H, and the average values of the corrosion rate as evaluated from the weight loss, P_W. In all cases $P_{i,EIS,UP}$ was significantly smaller than P_W.

Fig. 12(b) shows the result of fitting the EIS data to the RCL equivalent circuit. Similar to Fig. 12(a), in all cases $P_{i,RCL}$ was significantly smaller than P_W.

Fig. 13 presents a similar analysis for EIS data for specimens B2 and B3 from ingot B. In all cases the values of $P_{i,EIS,UP}$ and $P_{i,RCL}$ were significantly smaller than P_W.

Table 6 provides the corresponding values of the apparent valence for Mg corrosion given by

$$V_{W,UP} = \frac{2P_{i,EIS,UP}}{P_W} \tag{9}$$

based on the assumptions that $P_{i,EIS,UP}$ was a good measure of the amount of the corrosion rate under electrochemical influence, and that P_W was a good measure of the total corrosion rate. Similarly, the apparent valence, $V_{W,RCL}$ was evaluated substituting $P_{i,RCL}$ for $P_{i,EIS,UP}$ in Eq(9). In all cases the value of apparent valence was smaller than 2.0, and the values were all less than 1.0 with only the one exception.

An evaluation of the measurement errors was carried out by Cao et al [6,11]. This indicated that the maximum measurement error was less than 5% in the measurement of both P_W and P_H, whereas the maximum measurement error was 20 % in P_i and $P_{i,EIS}$. Thus, there is a significant difference between $P_{i,EIS,UP}$ and $P_{i,RCL}$ and P_H and P_W.

6. Discussion

The values of the corrosion rate measured by all the electrochemical methods discussed above all depend on the experimentally measured anodic Tafel slope, β_a. This has been evaluated herein by LEV fitting of the cathodic polarisation curves using Eq(4). Each of these values of the anodic Tafel slope was most probably an under-estimation.

Song et al [16,17] showed that the corrosion of pure Mg in chloride and sulphate solutions involved a partially protective film, and furthermore that there was increasing film breakdown with anodic polarisation from the open circuit potential, particularly in chloride solutions. Thus, it is expected [16,17,18] that the anodic current density, for an applied potential E, under conditions at which the cathodic partial reaction can be neglected, is given by

$$i_a = A_f\left(E, pH\right) i_{ao} \exp\left(\frac{\left(E - E_{ae}\right)}{\beta_{a0}}\right) \tag{10}$$

where $A_f(E, pH)$ is the film free area, i_{a0} is the exchange current density of the anodic partial reaction on the film free area, E_{ae} is the equilibrium potential for the anodic partial reaction, and β_{a0} is the Tafel constant for the anodic partial reaction on the film free area. Eq(10) indicates that the anodic partial reaction increases at a faster rate that expected from the anodic Tafel slope as would be evaluated by fitting Eq(4) to the cathodic polarization curve.

This means that each of the values of corrosion rate evaluated herein by an electrochemical EIS method is an over-estimate of the actual corrosion rate. As a consequence the values of the apparent valence for Mg are also over-estimates. In all cases, the apparent valence was less than 2.0, and in many cases the value of the apparent valence was less than 1.0.

A possible reason, as suggested by Atrens et al [12], is that the evolving hydrogen causes an isolation of part of the specimen from the electrochemical measurement system.

Fig. 14 shows how a bubble of hydrogen could isolate part of the corroding specimen from the electrochemical measurement system. Corrosion could occur under the hydrogen bubble with the local cathodic current density, i_{cl} balancing the local anodic current density, i_{al}.

Alternatively, it is possible that polarisation of Mg in chloride solutions may not be consistent with typical Tafel behaviour as described by Eq(4) involving only one anodic and one cathodic reaction, and as suggested by Song [19] in those cases the corrosion rate cannot be estimated by either anodic or cathodic extrapolation.

This reanalysis of our recent EIS data leads to conclusions similar to those in the original papers [3,6,10,11]. Consequently there is no experimental evidence that requires revision of the conclusions in those papers, or of the conclusions of our recent review [12].

10. Conclusions

1. Analysis fully in compliance with the suggestions of King et al [1], and using *iR* corrected values of the Tafel slopes, indicated that each value of the corrosion rate evaluated by an electrochemical method (i.e. from either EIS data or from Tafel extrapolation) was less than the corrosion rate evaluated by weight loss. This difference was significant.

2. The corrosion rates evaluated using EIS and the RCL equivalent circuit (i.e. the equivalent circuit proposed by King et al [1]) were comparable to those evaluated using the simple fitting (sf) in which the inductive loop in the low frequency range was simply fitted with a semi-circle.

3. The values of the corrosion evaluated from EIS data were typically not good measurements of the corrosion rate of Mg as measured by weight loss.

4. Values of the apparent valence were evaluated based on the assumption that the corrosion rates evaluated with an electrochemical technique (i.e. from either EIS data or Tafel extrapolation) were good measures of that part of the total corrosion rate that was under electrochemical control. The value of the apparent valence was in each case less than 2.0 and in many cases less than 1.0.

5. The low values of apparent valence for Mg corrosion could be caused by the evolving

hydrogen isolating part of the corroding Mg surface from the electrochemical measuring system.

6. Based on the analyses above, the conclusions of our recent papers [3,6,10,11] and our recent review [12] stand well, and are reasonable.

Symbols pertaining to corrosion rate

P_i instantaneous corrosion rate evaluated using Eq(3) from the corrosion current density, i_{corr}, which can be evaluated either (i) by Tafel extrapolation (or LEV extrapolation) of a polarisation curve, or (ii) from the polarisation resistance, R_P, from EIS data using Eq(1), in which case there also needs to be values of the anodic and cathodic Tafel slopes.

$P_{i,u}$ instantaneous corrosion rate evaluated using Eq(3) from the corrosion current density, i_{corr}, evaluated by Tafel extrapolation of an un-*iR*-compensated cathodic polarisation curve.

$P_{i,IRC}$ instantaneous corrosion rate evaluated using Eq(3) from the corrosion current density, i_{corr}, evaluated by LEV fitting of an *iR*-compensated cathodic polarisation curve.

$P_{i,EIS}$ instantaneous corrosion rate evaluated previously from EIS data, evaluated from the charge transfer resistance, R_t, as a good measure of the polarisation resistance, R_P, and using values of the Tafel slopes, β_a and β_c from un-*iR*-compensated cathodic polarisation curves.

$P_{i,EIS,LF}$ instantaneous corrosion rate evaluated previously from EIS data evaluated using the low frequency limit, $R_{P,LP}$, as a good measure of the polarisation resistance, R_P, and using values of the Tafel slopes, β_a and β_c from un-*iR*-compensated cathodic polarisation curves.

$P_{i,RCL}$ instantaneous corrosion rate evaluated from EIS data fitted using the RCL equivalent circuit to estimate $R_{P,0}$ as a good measure of the polarisation resistance, R_P, and using values of the Tafel slopes, β_a and β_c from *iR*-compensated cathodic polarisation curves.

$P_{i,EIS,sf}$ instantaneous corrosion rate evaluated previously from EIS data fitted using the simple fitting model to estimate $R_{P,0}$ as a good measure of the polarisation resistance, R_P, and using values of the Tafel slopes, β_a and β_c from *iR*-compensated cathodic polarisation curves.

$P_{i,EIS,UP}$ instantaneous corrosion rate evaluated previously from EIS data evaluated using $R_{P,0}$ or the low frequency limit, $R_{P,LP}$, as a good measure of the polarisation resistance, R_P, and using values of the Tafel slopes, β_a and β_c from *iR*-compensated cathodic polarisation curves.

P_H instantaneous corrosion rate evaluated from the slope of the hydrogen evolution volume versus time data.

$P_{H6.5}$ instantaneous corrosion rate evaluated from the slope of the hydrogen evolution volume versus time data on the 6.5 day of immersion.

P_W average corrosion rate measured from weight loss.

P_{AH} average corrosion rate measured from the total evolved hydrogen over the duration of the immersion test.

Acknowledgements

The support of the Australian Research Council Centre of Excellence Design of Light Alloys is acknowledged. The China Scholarship Council is thanked for providing a scholarship to Fuyong Cao.

References

1 A.D. King, N. Birbilis, J.R. Scully, Accurate Electrochemical Measurement of Magnesium Corrosion Rates; a Combined Impedance, Mass-Loss and Hydrogen Collection Study, Electrochim. Acta 121 (2014) 394-406.
2 W. Liu, F. Cao, A. Chen, L. Chang, J. Zhang, C. Cao, Corrosion behaviour of AM60 magnesium alloys containing Ce or La under thin electrolyte layers. Part 1: microstructure characteriszation and electrochemical behaviour, Corros. Sci. 52 (2010) 627-638.
3 Z. Qiao, Z. Shi, N. Hort, N. Zainal Abidin, A. Atrens, Corrosion behaviour of a nominally high purity Mg ingot produced by permanent mould direct chill casting, Corros. Sci. 61 (2012) 185-207.
4 M. Stern, A.L. Geary, Electrochemical Polarization I. A Theoretical Analysis of the Shape of Polarization curves, J Electrochem Soc, 104 (1957) 56-63.
5 D.A. Jones, Principles and prevention of corrosion, 2nd ed Prentice Hall, (1996)
6 F. Cao, Z. Shi, J. Hofstetter, P.J. Uggowitzer, G Song, M Liu, A Atrens, Corrosion of ultra-high-purity Mg in 3.5 % NaCl solution saturated with $Mg(OH)_2$, Corros. Sci. 75 (2013) 78-99.
7 Z. Shi, A. Atrens, An innovative specimen configuration for the study of Mg Corrosion, Corros. Sci. 53 (2011) 226-246.
8 J.R. Scully, Polarization resistance method for determination of instantaneous corrosion rates, Corrosion 56 (2000) 199-218.
9 W.J. Lorenz, F.M. Mansfield, Determination of corrosion rates by electrochemical; DC and AC methods, Corros. Sci. 21 (1981) 647-672.
10 Z. Shi, F. Cao, G.L. Song, M. Liu, A. Atrens, Corrosion behaviour in salt spray and in 3.5 % NaCl solution saturated with $Mg(OH)_2$ of as-cast and solution heat-treated binary Mg-RE alloys: RE = Ce, La, Nd, Y, Gd, Corros. Sci. 76 (2013) 98-118.
11 F. Cao, Z. Shi, G.L. Song, M. Liu, A. Atrens, Corrosion behaviour in salt spray and in 3.5 % NaCl solution saturated with $Mg(OH)_2$ of as-cast and solution heat-treated binary Mg-X alloys: X = Mn, Sn, Ca, Zn, Al, Zr, Si, Sr, Corros. Sci. 76 (2013) 60-97.
12 A. Atrens, G.L. Song, F. Cao, Z. Shi, P.K. Bowen, Advances in Mg corrosion and research suggestions, Journal of Magnesium and Alloys 1 (2013) 177-200.
13 P.E. Gill, W. Murray, Algorithms for the solution of the nonlinear least-squares problem, SIAM J. Numer. Anal. 15 (1978) 977-992.
14 K. Levenberg, A method for the solution of certain problems in least squares, Quart. Appl. Math. 2 (1944) 164-168
15 D.W. Marquardt, An algorithm for least-squares estimation of nonlinear parameters, SIAM J. Appl. Math. 11 (1963) 431-441.
16 G. Song, A. Atrens, D. StJohn, J. Nairn, Y. Li, The electrochemical corrosion of pure magnesium in 1 N NaCl, Corros. Sci. 39 (1997) 855-875.
17 G. Song, A. Atrens, D. StJohn, X. Wu, J. Nairn, The anodic dissolution of magnesium in chloride and sulphate solutions, Corros. Sci. 39 (1997) 1981-2004.

18 A.Atrens, Overview of Mg corrosion mechanism, ECS Transactions 50 (2013) 335-344.
19 G.L. Song, Corrosion electrochemistry of magnesium (Mg) and its alloys, in Corrosion of magnesium alloys, ed. G.L. Song, Woodhead (2011) 3-65.

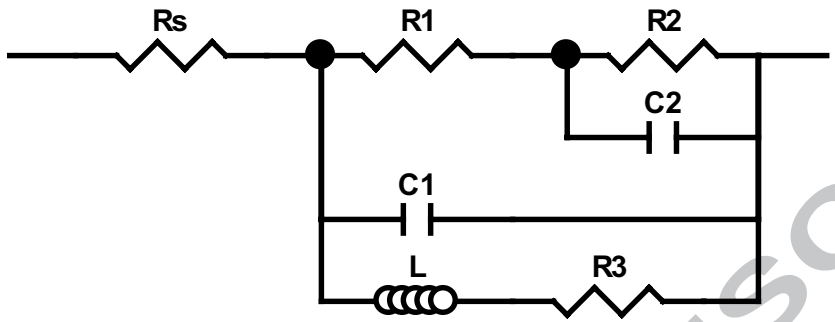

Fig. 1 Equivalent circuit proposed by King et al [1], designated herein as the RCL equivalent circuit.

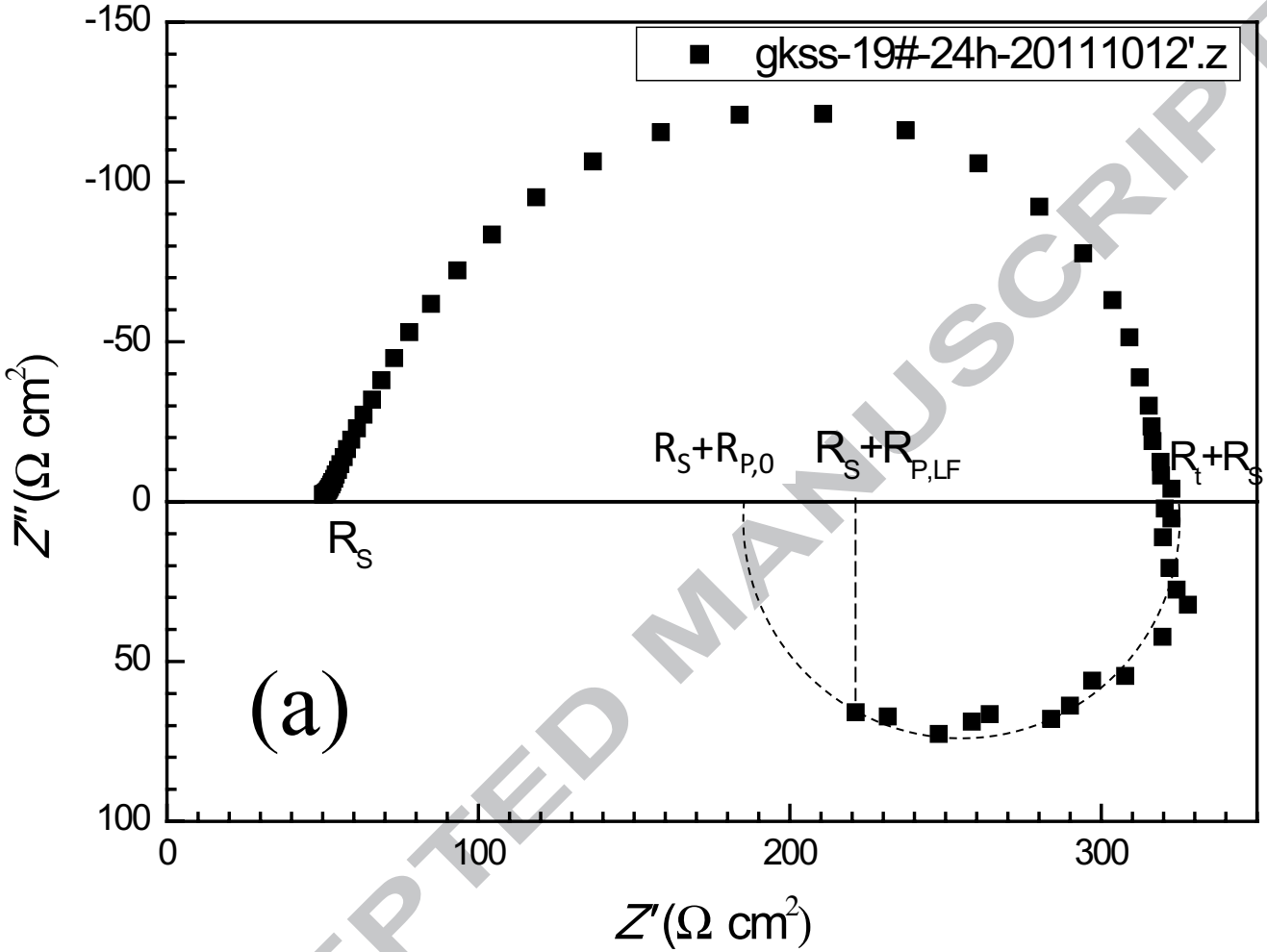

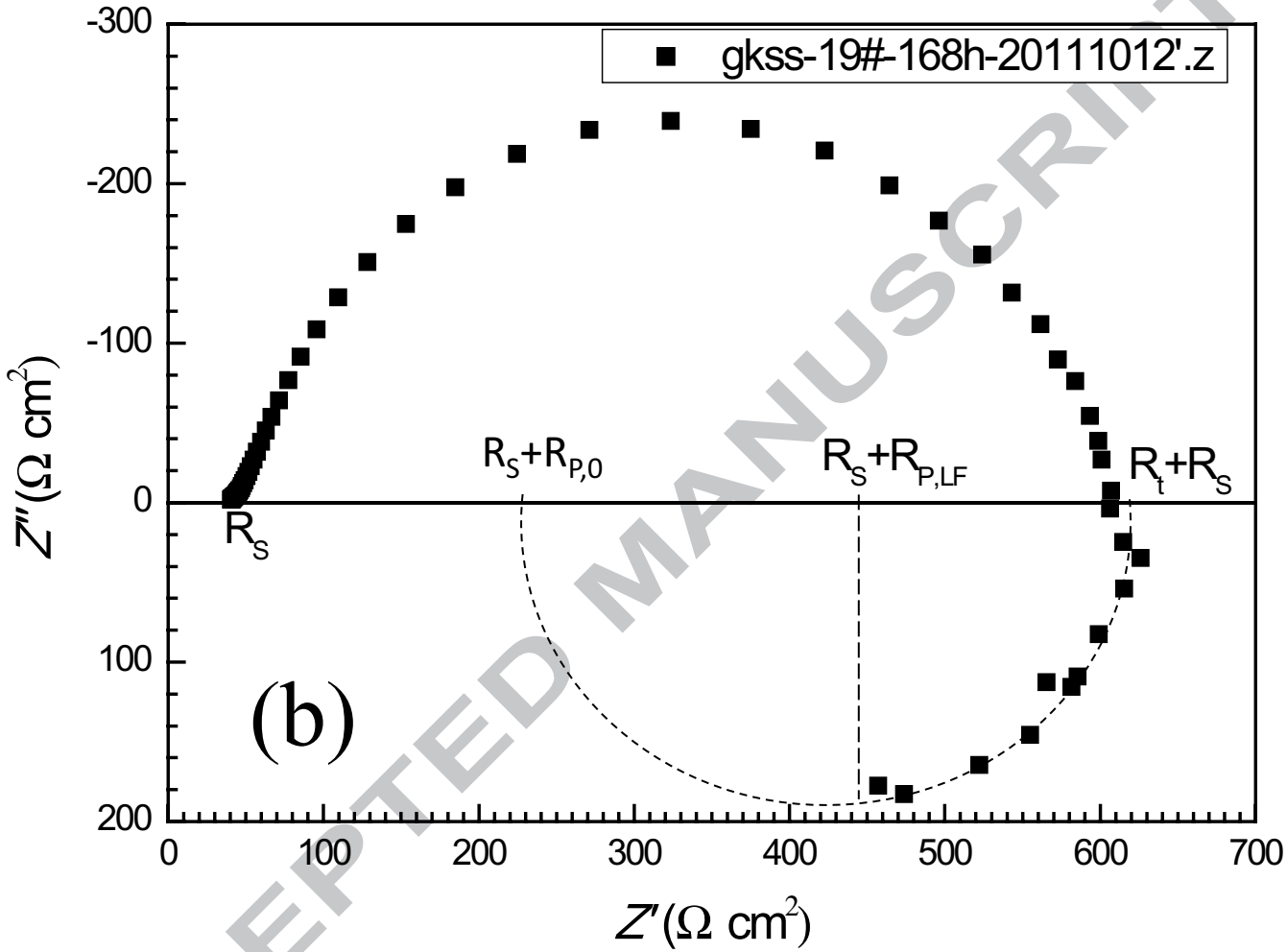

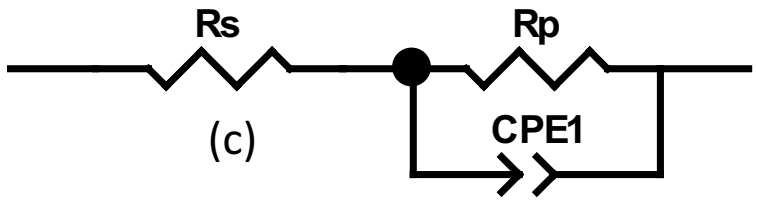

Fig. 2 Typical EIS data from Qiao et al [3] for a Mg specimen (specimen 19 in the notation of Qiao et al [3]) immersed at the open circuit potential in 3.5% NaCl solution saturated with $Mg(OH)_2$ at 25 œ2 ˚C. R_s is the solution resistance, R_t is the charge transfer resistance, and R_P is the polarisation resistance. King et al [1] pointed out that R_P needs to be evaluated at the low frequency (f) limit as the frequency approaches zero. This typically needs an *extrapolation* of the measured data. One simple extrapolation is shown by the dashed curve. The dashed curve shows a simple EIS data fitting by a semi-circle in the lower frequency range; (c) presents the equivalent circuit for this simple fitting. The EIS data were measured after (a) 1 day (24 h) immersion, and (b) 7 d (168 h) immersion in the solution.

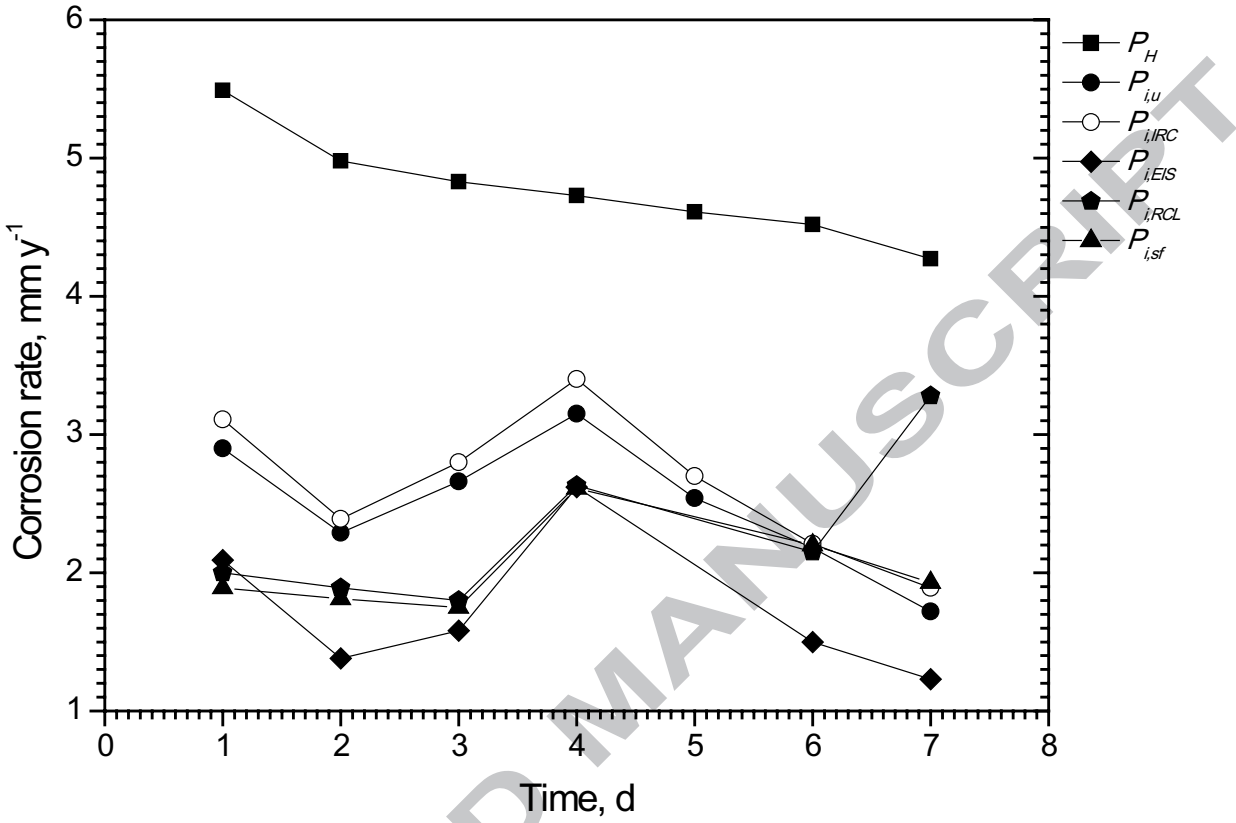

Fig. 3 Comparison of the instantaneous corrosion rate measured from hydrogen evolution, P_H, compared with corrosion rates measured by various electrochemical techniques, for Mg specimen 19 of Qiao et al [3] immersed at the open circuit potential in 3.5% NaCl solution saturated with $Mg(OH)_2$ at 25 œ2 ˚C.

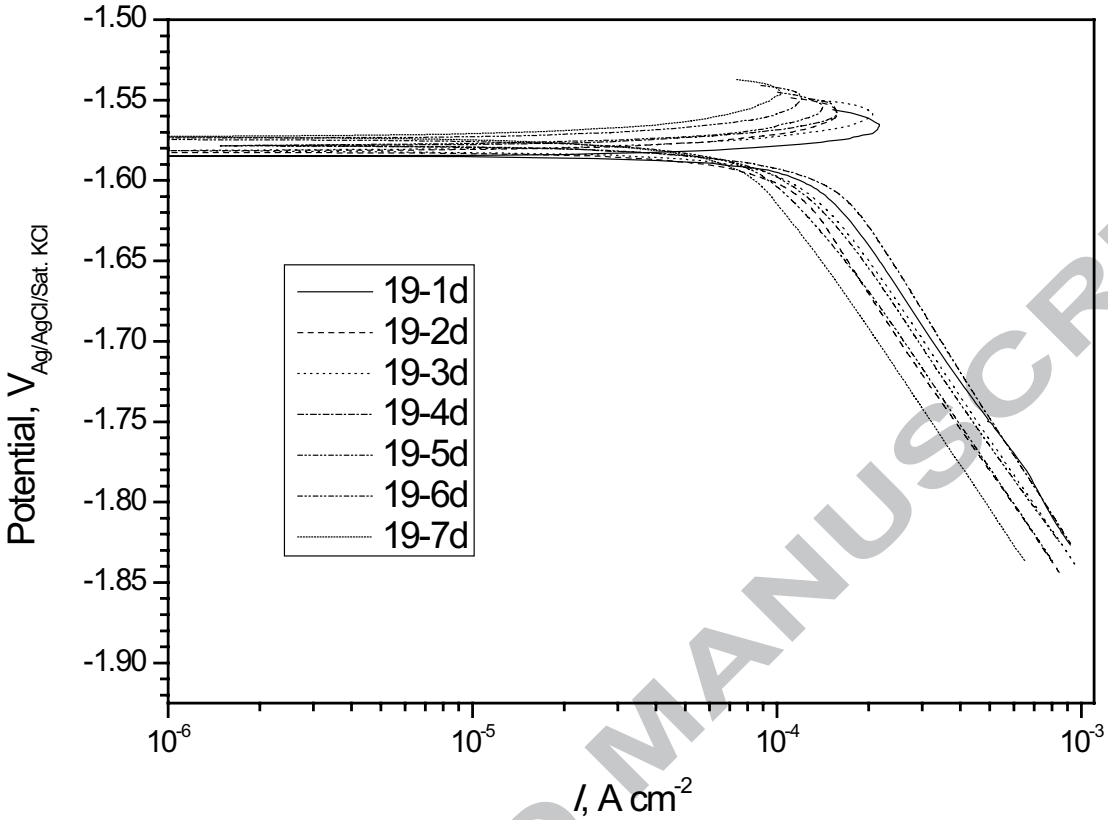

Fig. 4 Polarisation curves with *iR* compensation for Mg specimen 19 of Qiao et al [3] immersed at the open circuit potential in 3.5% NaCl solution saturated with $Mg(OH)_2$ at 25 œ2 ˚C.

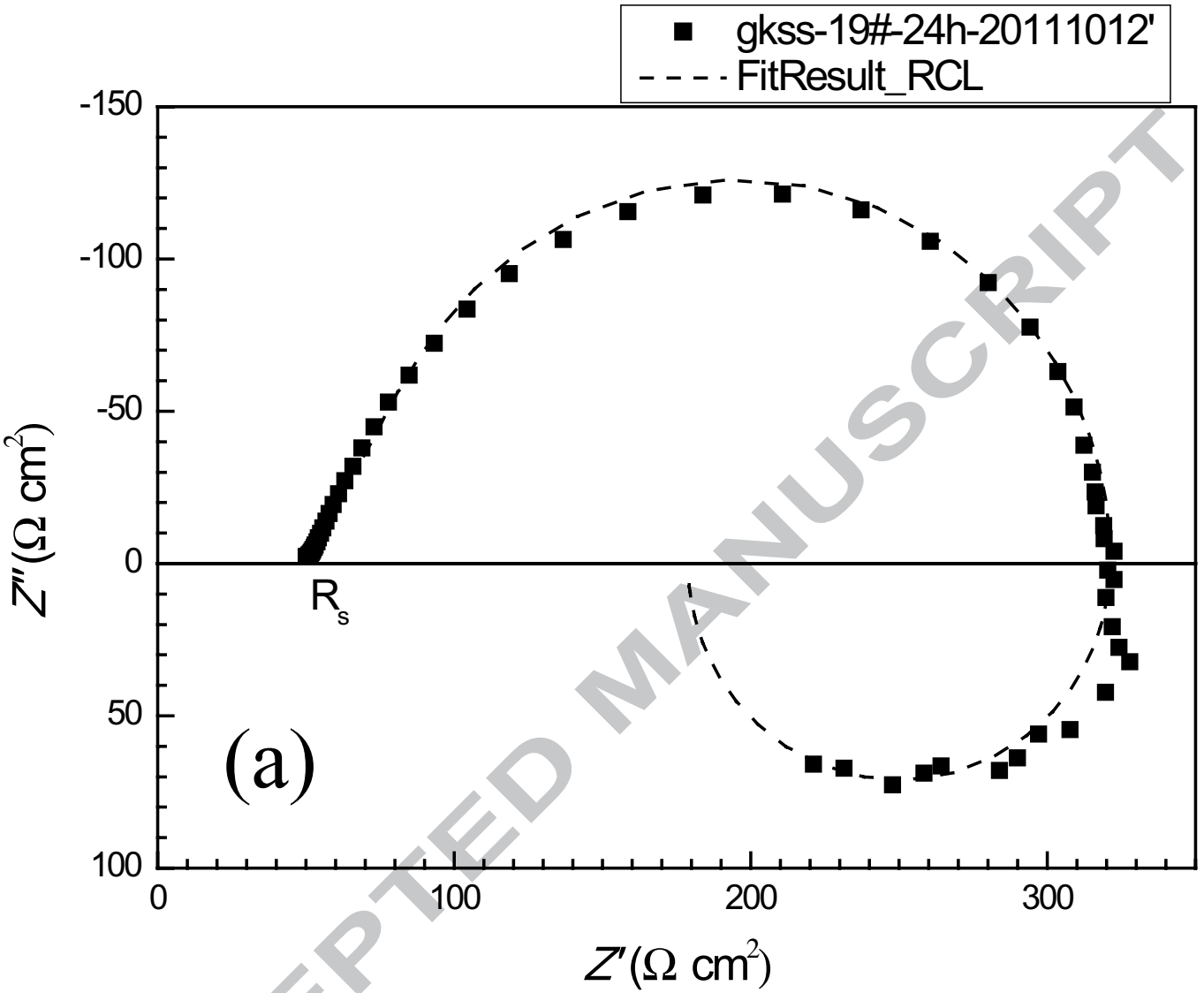

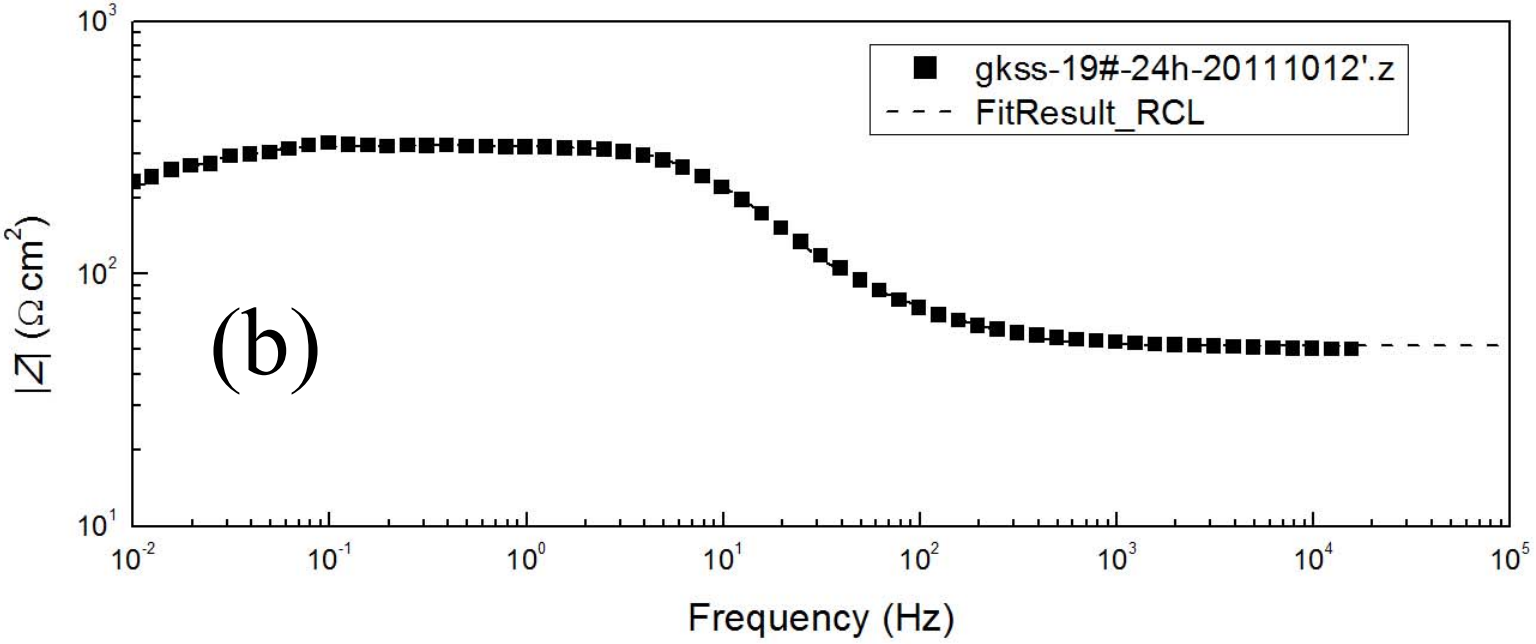

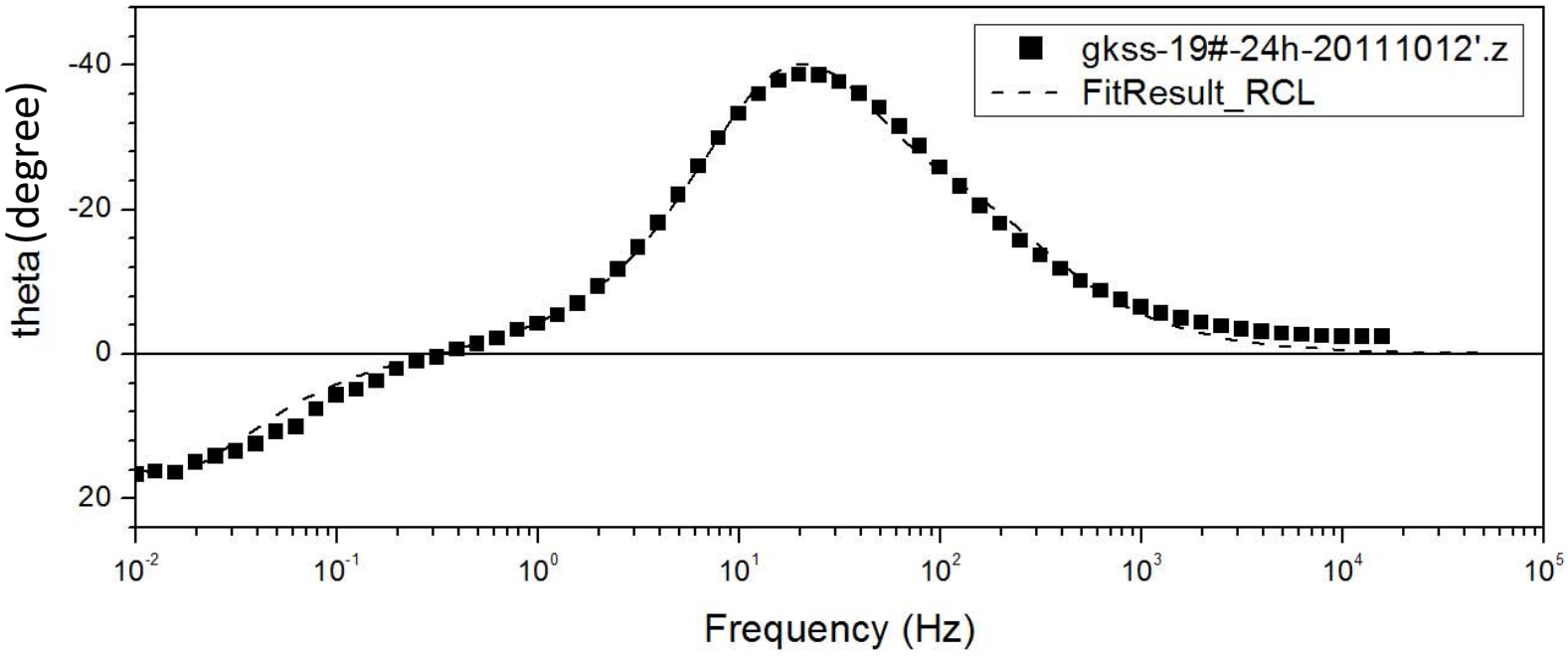

Fig. 5 Typical EIS data (data points) and curve fitting (dashed line) by the RCL equivalent circuit for Mg specimen 19 of Qiao et al [3] immersed at the open circuit potential in 3.5% NaCl solution saturated with $Mg(OH)_2$ at 25 œ 2 ˚C for 1 d, (a) Nyquist plot, (b) and (c) Bode plots.

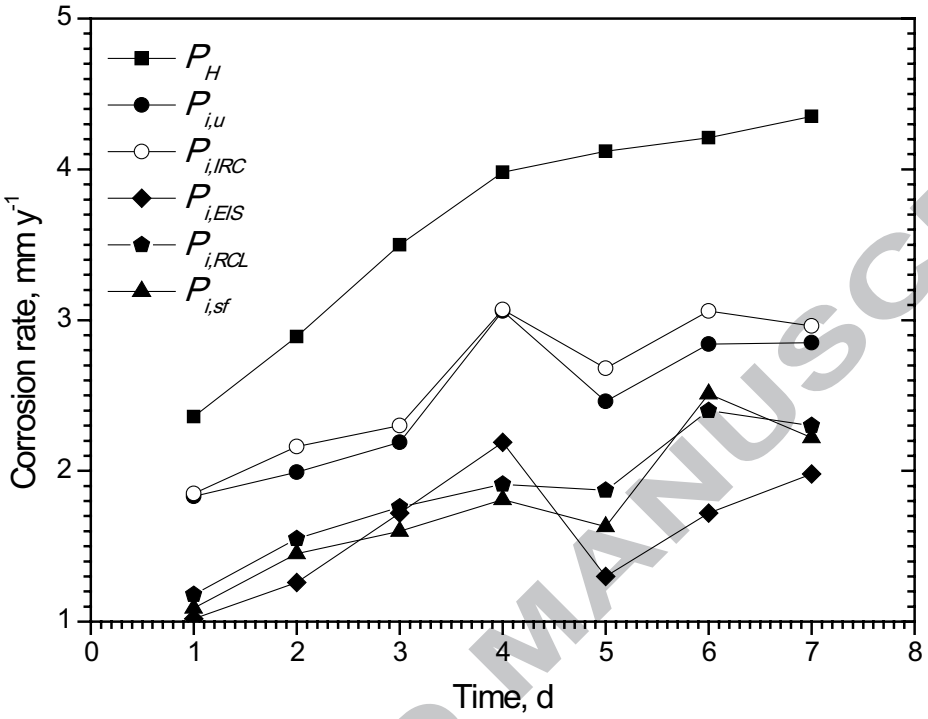

Fig. 6 Comparison of the instantaneous corrosion rate measured from hydrogen evolution, P_H, compared with corrosion rates measured by various electrochemical techniques, for Mg specimen 28 of Qiao et al [3] immersed at the open circuit potential in 3.5% NaCl solution saturated with $Mg(OH)_2$ at 25 œ2 ˚C for 7 days.

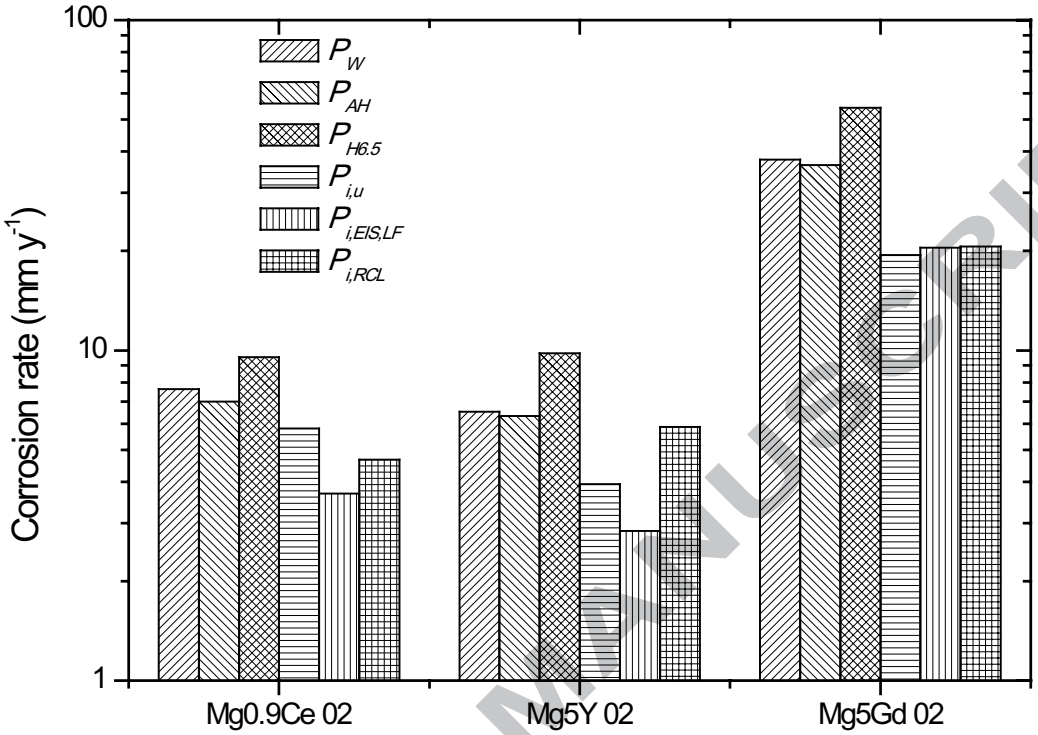

Fig. 7 Corrosion rates P_W, P_{AH}, $P_{H6.5}$, $P_{i,u}$, $P_{i,EIS,LF}$, and $P_{i,RCL}$ for solution heat-treated Mg0.9Ce, Mg5Y and Mg5Gd alloys in 3.5% NaCl solution saturated with $Mg(OH)_2$ for 7 days at 25 ± 2 °C, adapted from Shi et al [10]. $P_{i,u}$ and $P_{i,EIS,LF}$ were evaluated using the B value with no iR compensation. $P_{i,RCL}$ values were evaluated using the B value with iR compensation.

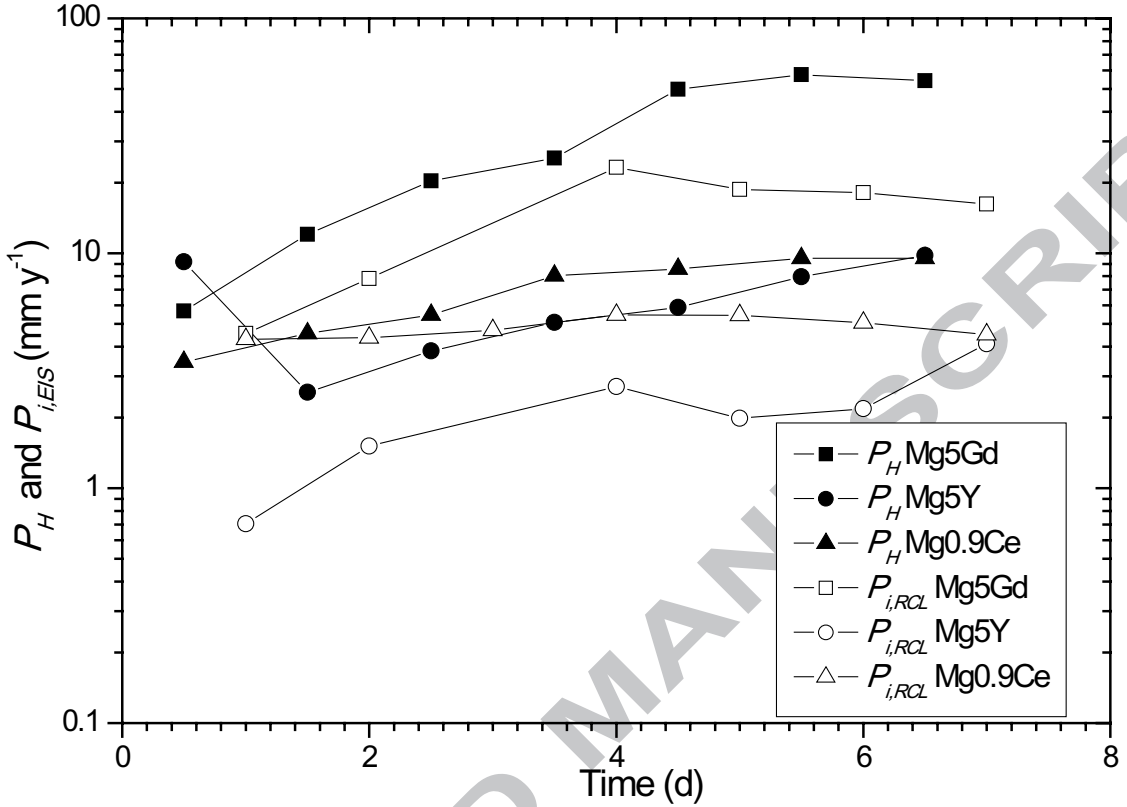

Fig. 8 Comparison of the instantaneous corrosion rates P_H and $P_{i,RCL}$ (fitted by the RCL equivalent circuit and using the *iR* corrected B value) for solution heat-treated Mg5Gd, Mg5Y and Mg0.9Ce alloys during immersion testing at the open circuit potential (OCP) in 3.5% NaCl solution saturated with $Mg(OH)_2$ for 7 days at 25 œ2 ˚C. Data were from Shi et al [10].

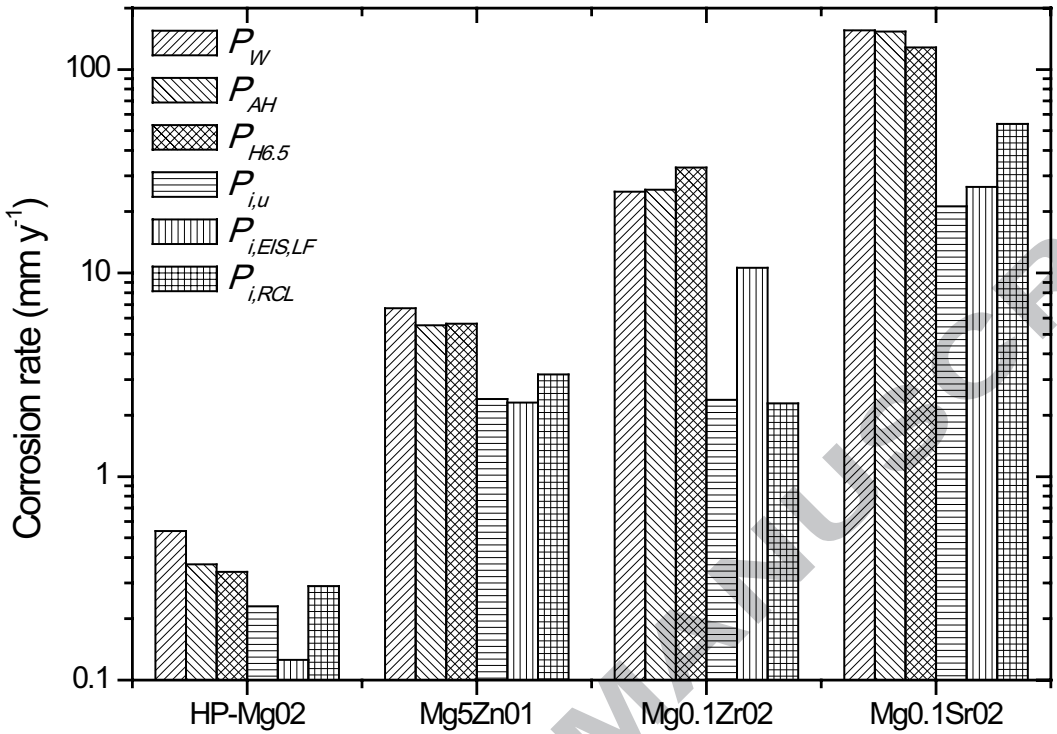

Fig. 9 Corrosion rates P_W, P_{AH}, $P_{H6.5}$, $P_{i.u}$, $P_{i,EIS,LF}$, and $P_{i,RCL}$ for as-cast high-purity magnesium and solution heat-treated Mg5Zn, Mg0.1Zr and Mg0.1Sr in 3.5% NaCl solution saturated with $Mg(OH)_2$ for 7 days at 25 œ2 ˚C, adapted from Cao et al [11]. $P_{i,u}$ and $P_{i,EIS,LF}$ were evaluated using the B value with no iR compensation. $P_{i,RCL}$ values were evaluated using the B value with iR compensation.

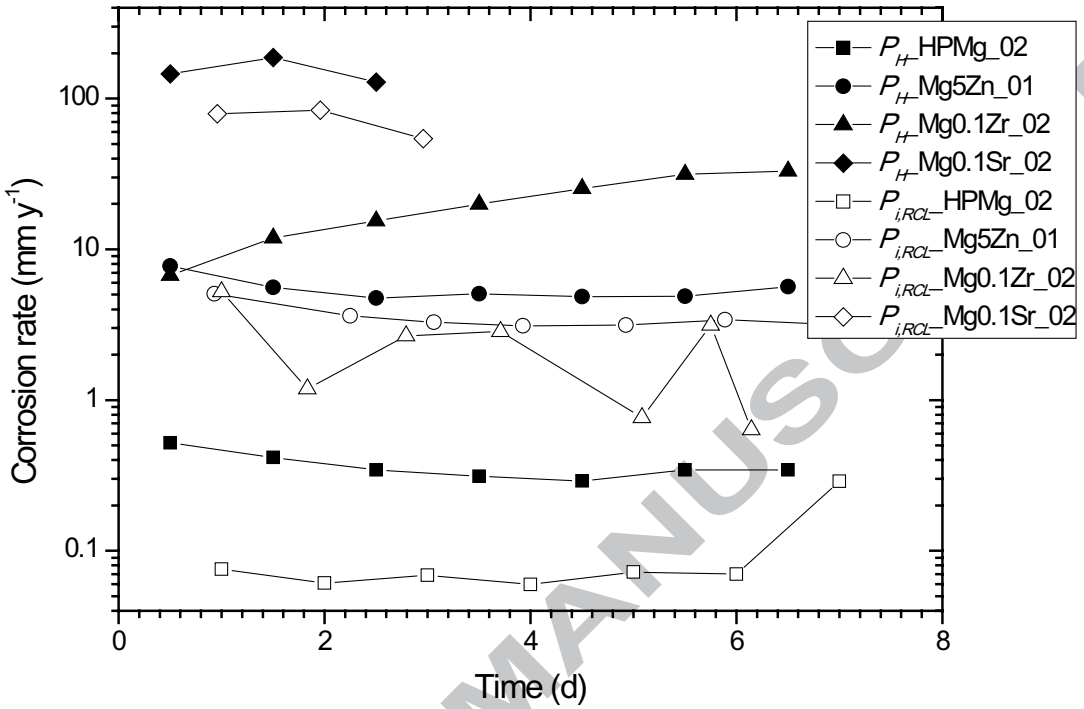

Fig. 10 Instantaneous corrosion rates P_H and $P_{i,RCL}$ (based on the RCL equivalent circuit and using the *iR* corrected B value) of as-cast high-purity magnesium and solution heat-treated Mg5Zn, Mg0.1Zr and Mg0.1Sr versus immersion time at the open circuit potential (OCP) in 3.5% NaCl solution saturated with $Mg(OH)_2$ for 7 days at 25 œ2 ˚C. The data were from Cao et al [11].

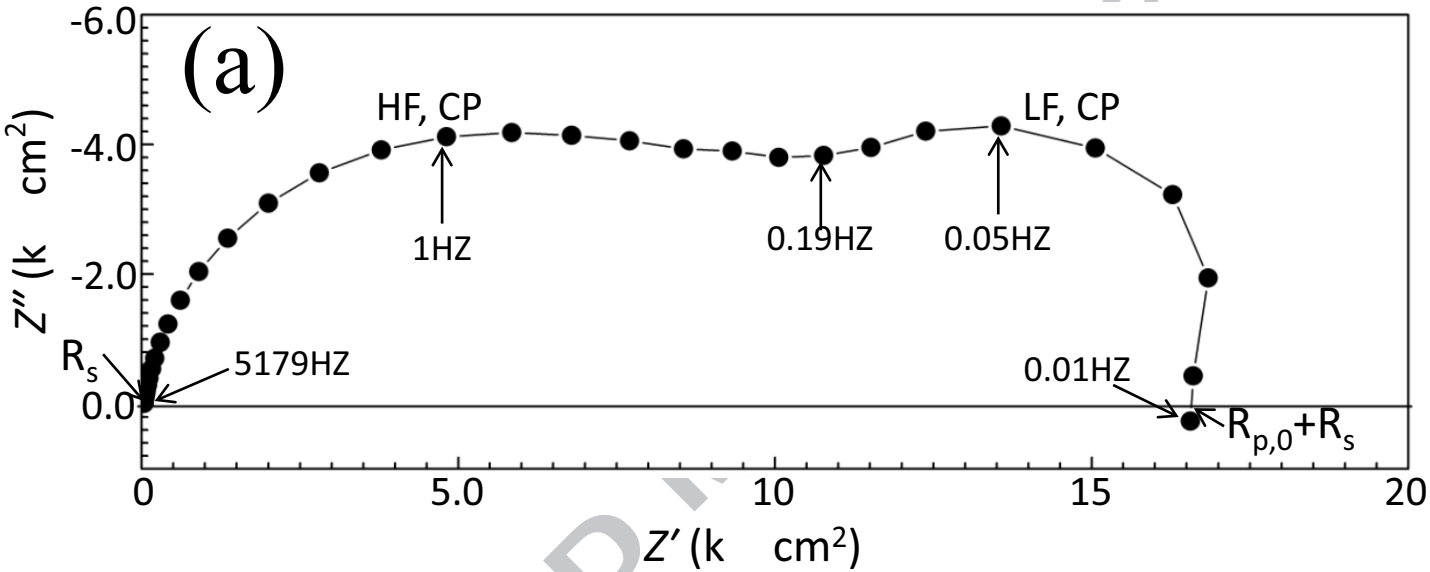

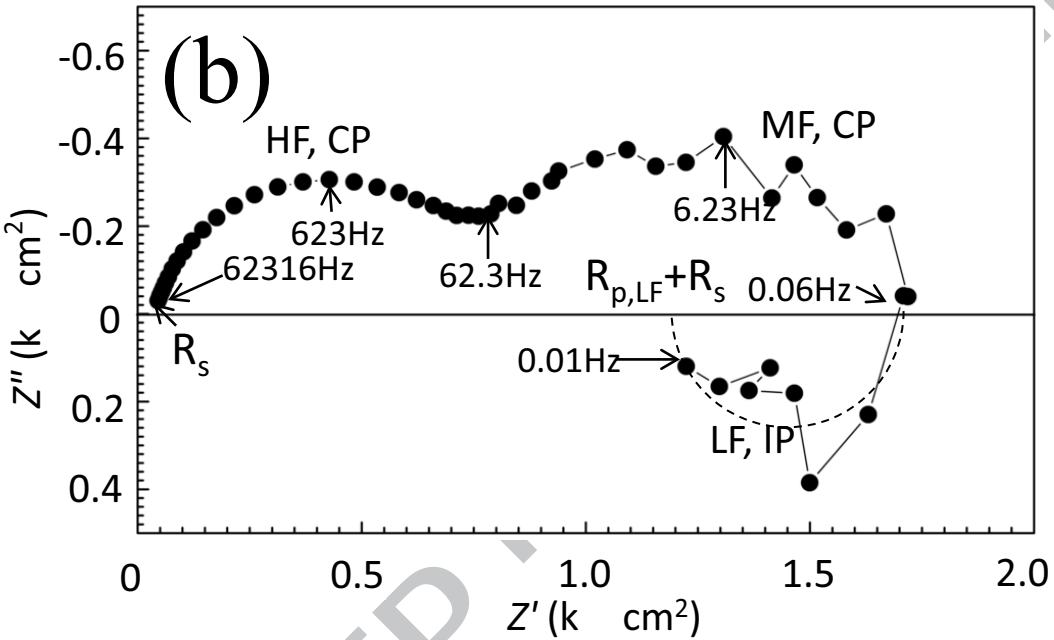

Fig. 11 Typical EIS data for for corrosion of UP Mg immersed at the open circuit potential in 3.5% NaCl solution saturated with $Mg(OH)_2$ at 25 œ2 ˚C adapted from Cao et al [6], (a) showing only two capacitive loops, and (b) showing two capacitive loops and an inductive loop.

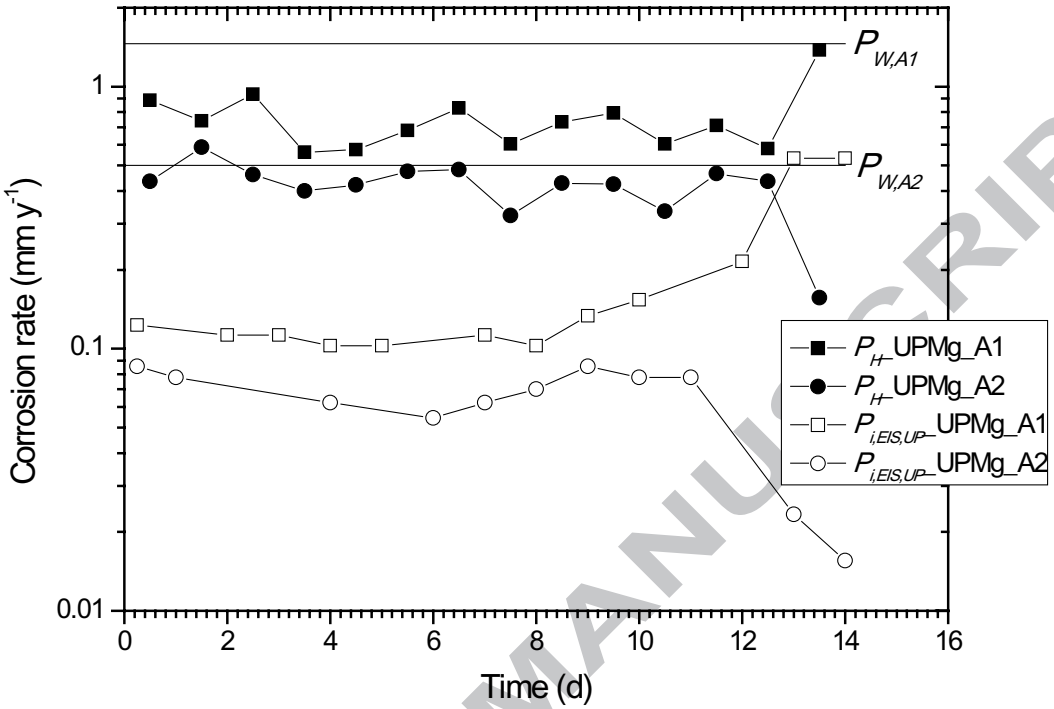

Fig. 12(a) Corrosion rates P_H and $P_{i,EIS,UP}$ (evaluated with B value with *iR* correction) of ultra-high-purity magnesium specimens A1 and A2 from ingot A versus immersion time at the open circuit potential (OCP) in 3.5% NaCl solution saturated with $Mg(OH)_2$ for 14 days at 25 œ2 ˚C. Data were from Cao et al [6].

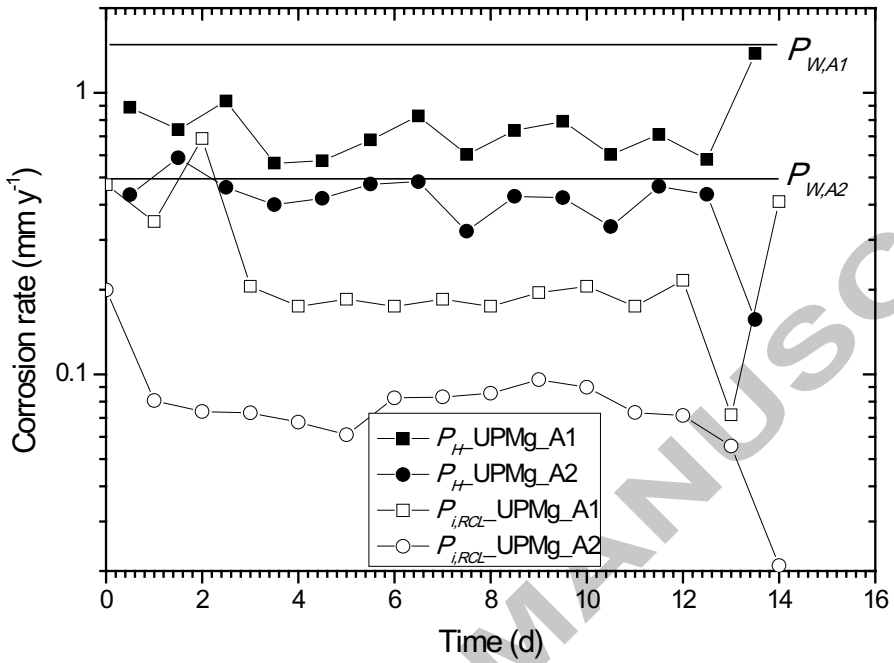

Fig. 12(b) Corrosion rates P_H and $P_{i,RCL}$ (with B value with iR correction) of ultra-high-purity magnesium specimens A1 and A2 of ingot A versus immersion time at the open circuit potential (OCP) in 3.5% NaCl solution saturated with $Mg(OH)_2$ for 14 days at 25 œ2 ˚C. Data were from Cao et al [6].

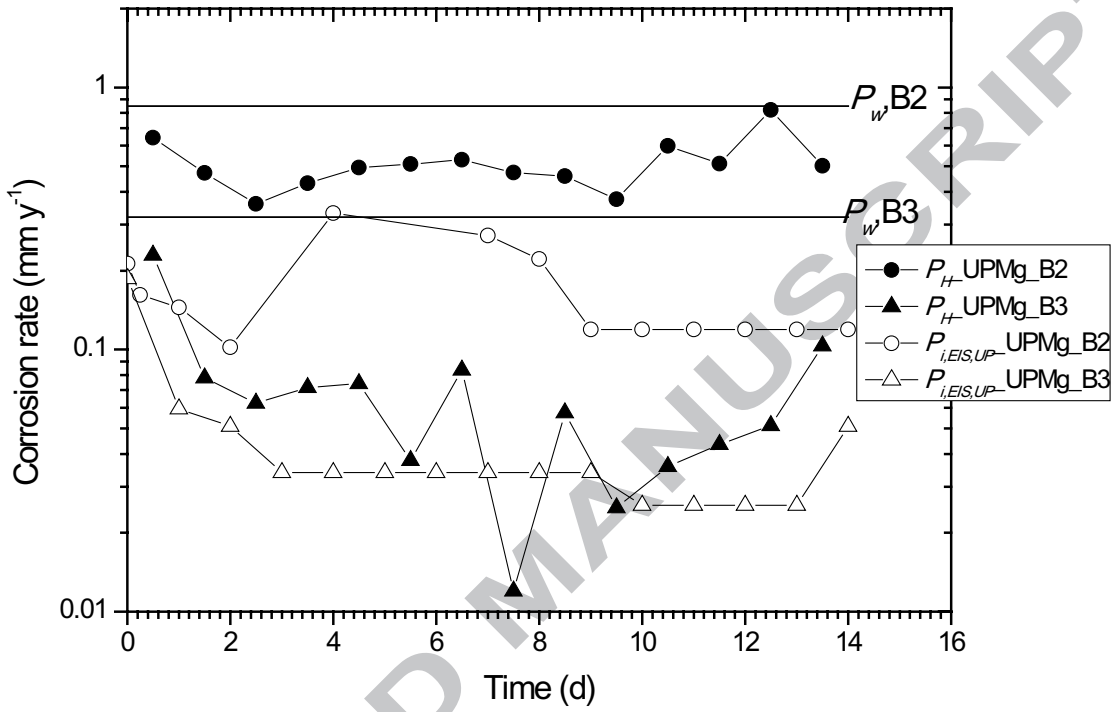

Fig. 13(a) Corrosion rates P_H and $P_{i,EIS,UP}$ (with B value with iR correction) of ultra-high-purity magnesium specimens B2 and B3 from ingot B versus immersion time at the open circuit potential (OCP) in 3.5% NaCl solution saturated with $Mg(OH)_2$ for 14 days at 25 œ2 ˚C. Data were from Cao et al [6].

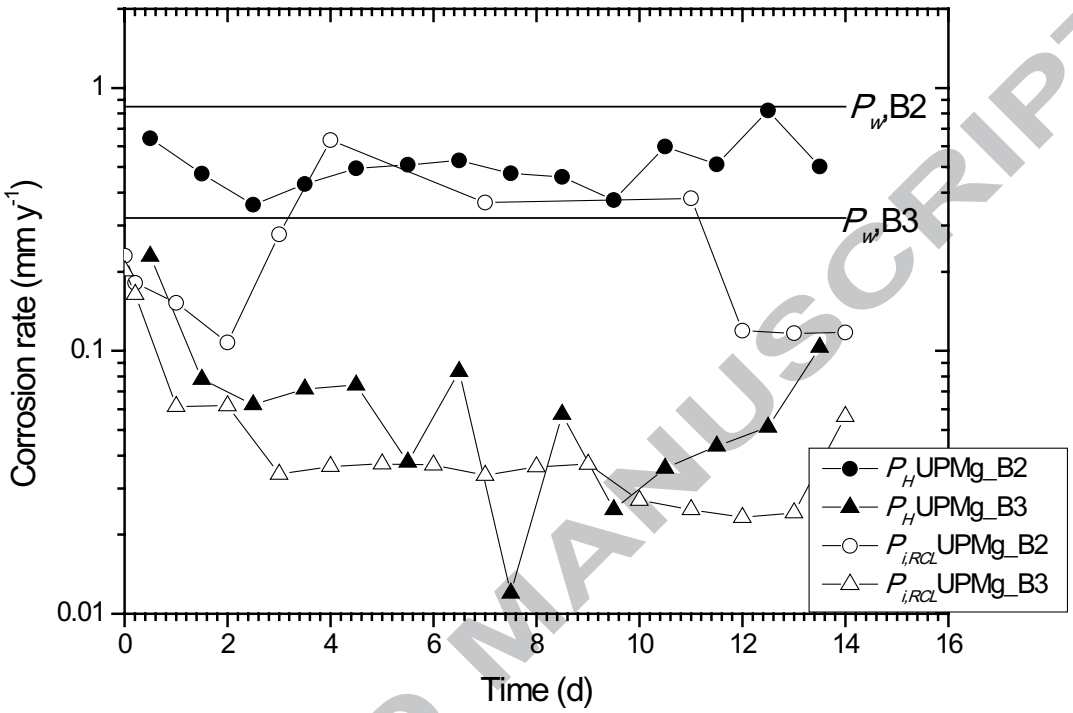

Fig. 13(b) Corrosion rates P_H and $P_{i,RCL}$ (with B value with *iR* correction) of ultra-purity magnesium specimens B2 and B3 from ingot B versus immersion time at the open circuit potential (OCP) in 3.5% NaCl solution saturated with $Mg(OH)_2$ for 14 days at 25 œ2 ˚C. Data were from Cao et al [6].

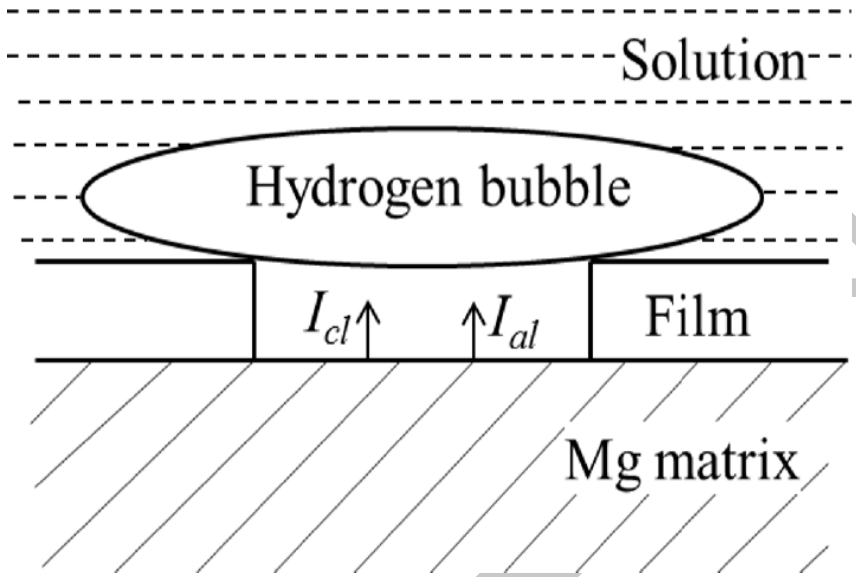

Fig. 14 A schematic following Atrens et al [12] shows how a bubble of hydrogen could isolate part of the corroding specimen from the electrochemical measurement system. Corrosion could occur under the hydrogen bubble with the local cathodic current density, i_{cl} balancing the local anodic current density, i_{al}.

Table 1. Parameters evaluated from the cathodic polarization curves, with no *iR* compensation designated as (no *iR*), and with *iR* compensation designated as (with *iR*) for Mg specimen 19 of Qiao et al [3], immersed for 7 days in 3.5% NaCl solution saturated with $Mg(OH)_2$ at 25 ± 2 °C.

Immersion Time d	E_{corr} $V_{Ag/AgCl/Sat.\ KCl}$	LEV (no *iR* compensation)				Tafel fitting (no *iR*)			LEV (with *iR* compensation)				Tafel fitting (with *iR*)		
		β_a mV decade^{-1}	β_c mV decade^{-1}	i_{corr} µA cm^{-2}	$P_{i,u}$ mm y^{-1}	β_c mV decade^{-1}	i_{corr} µA cm^{-2}	$P_{i,u}$ mm y^{-1}	β_a mV decade^{-1}	β_c mV decade^{-1}	i_{corr} µA cm^{-2}	$P_{i,IRC}$ mm y^{-1}	β_c mV decade^{-1}	i_{corr} µA cm^{-2}	$P_{i,IRC}$ mm y^{-1}
1	-1.585	48	-321	127	2.9	-334	131	3.0	28	-296	136	3.1	-271	123	2.8
2	-1.582	45	-312	100	2.3	-310	98.8	2.3	38	-294	105	2.4	-277	95.6	2.2
3	-1.581	48	-314	116	2.7	-318	119	2.7	38	-295	122	2.8	-280	114	2.6
4	-1.578	60	-349	138	3.2	-355	140	3.2	46	-321	149	3.4	-300	136	3.1
5	-1.578	60	-327	111	2.5	-326	109	2.5	53	-312	118	2.7	-290	106	2.4
6	-1.574	58	-313	96	2.2	-312	94.8	2.2	48	-289	97	2.2	-277	91	2.1
7	-1.572	56	-304	75	1.7	-311	77.3	1.8	54	-301	83	1.9	-279	74	1.7
Average	-1.579	54	-320	109	2.5	-324	110	2.5	44	-301	116	2.6	-281	106	2.4

Table 2. Parameters evaluated from the cathodic polarization curves and EIS, compared with the hydrogen evolution data, for Mg specimen 19 of Qiao et al [3], immersed for 7 days in 3.5% NaCl solution saturated with $Mg(OH)_2$ at 25 ± 2 °C.

Immersion Time d	E_{corr} $V_{Ag/AgCl/Sat.\ KCl}$	R_s	P_H	$P_{i,IRC}$	EIS	$V_{H,IRC}$				$V_{H,RCL}$	
		Ω cm^2	mm y^{-1}	mm y^{-1}	$P_{i,EIS}$	$R_{p,sf}$ Ω cm^2	$P_{i,sf}$ mm y^{-1}	$R_{p,RCL}$ Ω	$P_{i,RCL}$ mm y^{-1}		
1	-1.585	53	5.5	3.1	2.1	135	1.9	127	2.0	1.1	0.72
2	-1.582	36	5.0	2.4	1.4	184	1.8	177	1.9	0.96	0.76
3	-1.581	36	4.8	2.8	1.6	191	1.8	186	1.8	1.2	0.75
4	-1.578	51	4.7	3.4	2.6	153	2.6	152	2.6	1.4	1.1
5	-1.578	38	4.6	2.7	1.8	---	---	---	---	1.2	
6	-1.574	38	4.5	2.2	1.5	186	2.2	191	2.2	0.98	0.98
7	-1.572	41	4.3	1.9	1.2	236	1.9	139	3.3	0.88	1.5
Average	-1.579		4.8	2.6	1.7	165	2.7	147	3.1	1.1	1.3

Table 3. Parameters evaluated from the cathodic polarization curves and EIS, compared with the hydrogen evolution data, for Mg specimen 28 of Qiao et al [3], immersed for 7 days in 3.5% NaCl solution saturated with $Mg(OH)_2$ at 25 ± 2 °C.

Immersion Time d	E_{corr} $V_{Ag/AgCl/Sat. KCl}$	R_s	P_H mm y^{-1}	$P_{i,IRC}$ mm y^{-1}	EIS					$V_{H,IRC}$	$V_{H,RCL}$
		Ω cm^2			$P_{i,EIS}$	$R_{p,sf}$ Ω cm^2	$P_{i,sf}$ mm y^{-1}	$R_{p,RCL}$ Ω	$P_{i,RCL}$ mm y^{-1}		
1	-1.585	27	2.36	1.9	1.0	347	1.1	320	1.2	1.6	1.0
2	-1.582	25	2.89	2.2	1.3	297	1.5	277	1.6	1.5	1.1
3	-1.581	50	3.50	2.3	1.7	276	1.6	252	1.8	1.3	1.0
4	-1.578	34	3.98	3.1	2.2	213	1.8	201	1.9	1.6	0.95
5	-1.578	28	4.12	2.7	1.3	212	1.6	183	1.9	1.3	0.92
6	-1.574	28	4.21	3.1	1.7	158	2.5	166	2.4	1.5	1.1
7	-1.572	44	4.35	3.0	2.0	169	2.2	163	2.3	1.4	1.1
Average	-1.579		3.63	2.6	1.6	239	1.8	223	1.9	1.4	1.0

Table 4. Calculation of Stern-Geary Coefficient B was based on the data fitting (LEV) of the polarisation curve, without (β_a, β_c, B) and with iR compensation (β_{aIRC}, β_{cIRC}, B_{IRC}) of the polarisation curves.

	Mg0.9Ce	Mg5Y	Mg5Gd	HPMg	Mg5Zn	Mg0.1Zr	Mg0.1Sr
β_a (mV)	80	80	120	50	40	220	180
β_c (mV)	-350	-290	-350	-210	-206	-424	-378
B (mV)	28.3	27.3	38.9	17.3	15	63	53
R_s (Ω cm^{-2})	70	36.8	21.4	40.9	27.1	26.7	30.7
β_{aIRC} (mV)	46	76	90	41	60	214	65
β_{cIRC} (mV)	-228	-257	-250	-229	-174	-401	-277
B_{IRC} (mV)	16.6	25.5	28.8	15	19.4	60.7	23.2

Table 5(a). Values of apparent valence, $V_{H,RCL} = 2P_{i,RCL} / P_H$, for specimens Mg5Gd, Mg5Y, Mg0.9Ce, and HPMg02, immersed in 3.5% NaCl solution saturated with $Mg(OH)_2$ at 25 ± 2 °C corresponding to the data in Fig. 8.

Time	$P_{i,RCL}$				$V_{H,RCL}$			
(d)	Mg5Gd	Mg5Y	Mg0.9Ce	HPMg02	Mg5Gd	Mg5Y	Mg0.9Ce	HPMg02
1	4.6	0.71	4.3	0.08	1.60	0.15	2.50	0.29
2	7.8	1.5	4.7	0.06	1.30	1.18	1.92	0.29
3	--	--	4.7	0.07			1.72	0.40
4	23	2.7	5.5	0.06	1.83	1.07	1.36	0.38
5	19	2.0	5.4	0.07	0.75	0.68	1.27	0.49
6	18	2.2	5.1	0.07	0.63	0.55	1.06	0.41
7	16	4.1	4.5	0.29	0.60	0.84	0.95	1.68

Table 5(b). Values of apparent valence, $V_{H,RCL} = 2P_{i,RCL} / P_H$, for specimens Mg5Zn, Mg0.1Zr, Mg0.1Sr, and HPMg02, immersed in 3.5% NaCl solution saturated with $Mg(OH)_2$ at 25 ± 2 °C corresponding to the data in Fig. 10.

Time	$P_{i,RCL}$				$V_{H,RCL}$			
(d)	Mg5Zn	Mg0.1Zr	Mg0.1Sr	HPMg02	Mg5Zn	Mg0.1Zr	Mg0.1Sr	HPMg02
1	5.1	5.2	79	0.08	1.3	1.6	1.09	0.29
2	3.6	1.2	84	0.06	1.3	0.20	0.89	0.29
3	3.3	2.7	54	0.07	1.4	0.35	0.84	0.40
4	3.1	2.9		0.06	1.2	0.29		0.38
5	3.2	0.76		0.07	1.3	0.06		0.49
6	3.4	3.1		0.07	1.4	0.20		0.41
7	3.2	0.64		0.29	1.1	0.04		1.7

Table 6. Values of apparent valence, $V_{W,UP} = 2P_{i,EIS,UP}/P_W$ and $V_{W,RCL} = 2P_{i,RCL}/P_W$, corresponding to the data in Figs. 12 and 13, for corrosion of specimens A1, A2, B2 and B3 of ultra-high-purity Mg immersed at the open circuit potential (OCP) in 3.5% NaCl solution saturated with $Mg(OH)_2$ for 14 days at 25 ± 2 ˚C, data from Cao et al [6].

Time	$P_{i,EIS,UP}$				$P_{i,RCL}$				$V_{W,UP}$				$V_{W,RCL}$			
(d)	A1	A2	B2	B3	A1	A2	B2	B3	A1	A2	B2	B3	A1	A2	B2	B3
1	--	--	0.14	0.06	0.35	0.08	0.15	0.06	--	--	0.34	0.37	0.48	0.32	0.36	0.38
2	0.11	0.08	0.10	0.05	0.69	0.07	0.11	0.06	0.15	0.31	0.24	0.32	0.94	0.29	0.25	0.39
3	0.11	0.06	--	0.03	0.21	0.07	0.28	0.03	0.15	0.25	--	0.21	0.28	0.29	0.65	0.21
4	0.1	0.05	0.33	0.03	0.17	0.07	0.63	0.04	0.14	0.22	0.78	0.21	0.24	0.27	1.49	0.23
5	0.1	0.06	--	0.03	0.18	0.06	--	0.04	0.14	0.25	--	0.21	0.25	0.24	--	0.23
6	--	--	--	0.03	0.17	0.08	--	0.04	--	--	--	0.21	0.24	0.33	--	0.23
7	0.11	0.07	0.27	0.03	0.18	0.08	0.37	0.03	0.15	0.28	0.64	0.21	0.25	0.33	0.86	0.21
8	0.1	0.09	0.22	0.03	0.17	0.09	--	0.04	0.14	0.34	0.52	0.21	0.24	0.34	--	0.23
9	0.13	0.08	0.12	0.03	0.19	0.10	--	0.04	0.18	0.31	0.28	0.21	0.27	0.38	--	0.23
10	0.15	0.08	0.12	0.03	0.21	0.09	--	0.03	0.21	0.31	0.28	0.16	0.28	0.36	--	0.17
11	--	--	0.12	0.03	0.17	0.07	0.38	0.02	--	--	0.28	0.16	0.24	0.29	0.90	0.16
12	0.22	--	0.12	0.03	0.22	0.07	0.12	0.02	0.30	--	0.28	0.16	0.30	0.29	0.28	0.15
13	0.53	0.02	0.12	0.03	0.07	0.06	0.12	0.02	0.73	0.09	0.28	0.16	0.10	0.22	0.27	0.15
14	0.53	0.02	0.12	0.05	0.41	0.02	0.12	0.06	0.73	0.06	0.28	0.32	0.56	0.08	0.28	0.35

Table 7. Comparison of the parameters fitting the polarisation curves without *iR* drop correction (β_a, β_c, B) and with *iR* drop correction (β_{aIRC}, β_{cIRC}, B_{IRC}) for the corrosion of ultra-high-purity magnesium specimens A1, A2, B2, and B3 at the open circuit potential (OCP) in 3.5% NaCl solution saturated with $Mg(OH)_2$ for 14 days at 25 ± 2 ˚C, data from Cao et al [6].

	A1	A2	B2	B3
β_a (mV)	82	120	244	270
β_c (mV)	-260	-183	-209	-168
B (mV)	27.2	31.5	48.9	45
R_s (Ω cm^{-2})	37	50	108	38
β_{aIRC} (mV)	80	66	198	230
β_{cIRC} (mV)	-327	-387	-185	-142
B_{IRC} (mV)	27.9	24.5	41.6	38.2

Highlights

- Data reanalysis confirmed prior conclusions.
- EIS data did not provide good measurements of the corrosion rate.
- Electrochemical evaluated corrosion rates were less than those evaluated by weight loss.
- The value of the apparent valence was in many cases less than 1.0.
- Part of the corrosion may be isolated by hydrogen gas from electrochemical measurement.